J. Membrane Biol. 153, 181–194 (1996)

The Journal of
Membrane
Biology

Sugar Transport Heterogeneity in the Kidney: Two Independent Transporters or Different Transport Modes through an Oligomeric Protein? 1. Glucose Transport Studies

N. Oulianova, A. Berteloot

Membrane Transport Research Group, Department of Physiology, Faculty of Medicine, Université de Montreal, CP 6128, succursale ''Centre-Ville,'' Montreal (Québec) Canada H3C 3J7

Received: 25 October 1995/Revised: 10 June 1996

Abstract. The kinetics of Na^+/D-glucose cotransport (SGLT) were reevaluated in rabbit renal brush border membrane vesicles isolated from the whole kidney cortex using a fast-sampling, rapid-filtration apparatus (FSRFA, US patent #5,330,717) for uptake measurements. Our results confirm SGLT heterogeneity in this preparation, and both high (HAG) and low (LAG) affinity glucose transport pathways can be separated over the 15–30°C range of temperatures. It is further shown that: (i) Na^+ is an essential activator of both HAG and LAG; (ii) similar energies of activation can be estimated from the linear Arrhenius plots constructed from the V_{max} data of HAG and LAG, thus suggesting that the lipid composition and/or the physical state of the membrane do not affect much the functioning of SGLT; (iii) similar V_{max} values are observed for glucose and galactose transport through HAG and LAG, thus demonstrating that the two substrates share the same carrier agencies; and (iv) phlorizin inhibits both HAG and LAG competitively and with equal potency ($K_i = 15$ μM). Individually, these data do not allow us to resolve conclusively whether the kinetic heterogeneity of SGLT results from the expression in the proximal tubule of either two independent transporters (rSGLT1 and rSGLT2) or from a unique transporter (rSGLT1) showing allosteric kinetics. Altogether and compared to the kinetic characteristics of the cloned SGLT1 and SGLT2 systems, they do point to a number of inconsistencies that lead us to conclude the latter possibility, although it is recognized that the two alternatives are not mutually exclusive. It is further suggested, from the differences in the K_m values of HAG transport in the kidney as compared to the small intestine and SGLT1 cRNA-injected oocytes, that renal SGLT1 activity is somehow modulated, maybe through heteroassociation with (a) regulatory subunit(s) that might also contribute quite significantly to sugar transport heterogeneity in the kidney proximal tubule.

Key words: Na^+-dependent sugar transport — Substrate specificity — Phlorizin inhibition — Temperature dependence — Membrane vesicles (rabbit kidney)

Introduction

In the ''Na^+ gradient hypothesis'' regarding transcellular absorption of sugars by intestinal and renal epithelial cells [15], glucose is first accumulated within the cell by secondary active transport through the apical brush border membrane (BBM).[1] Over the last 25 years, studies using BBM vesicles (BBMV) [6, 51, 53, 69] and isolated cells [26] have greatly contributed to the characterization of Na^+-dependent D-glucose cotransport (SGLT) in terms of substrate and inhibitor specificities, Na^+ activation, membrane potential dependency, and mechanism of cotransport. It has been generally assumed, up to the early eighties, that SGLT expression in mammals is homogeneous [15]. However, the studies of Barfuss and Schafer [1] using the isolated perfused tubule technique, and those of Turner and Moran [59–61] in renal BBMV,

Correspondence to: A. Berteloot

[1] Abbreviations: AMG: α-methylglucose; BBM: brush border membrane; BBMV: brush border membrane vesicles; BCA: bicinchoninic acid; EDTA: ethylenediaminetetraacetic acid; FSRFA: fast-sampling, rapid-filtration apparatus; HAG: high affinity glucose; HAP: high affinity phlorizin; HEPES: N-[2-hydroxyethyl]piperazine-N′-[2-ethanesulfonic acid]; LAG: low affinity glucose; LAP: low affinity phlorizin; SER: standard error of regression; SGLT: Na^+/D-glucose cotransport; Tris: tris[hydroxymethyl]aminomethane.

which both demonstrated kinetic heterogeneity of SGLT along the rabbit proximal tubule, seem to have put a definitive end to this assumption. Still, the molecular basis of this heterogeneity has not been firmly established yet.

Genetic defects of SGLT systems are expressed in selective congenital glucose/galactose malabsorption by the small intestine and familial renal glycosuria, and a minimum of two SGLT genes appear necessary to explain the clinical findings [16, 50]. The studies of Turner and Moran [59–61] were interpreted along these lines and it was concluded that there exists both high-affinity glucose (HAG, $K_m = 0.35$ mM) and low-affinity glucose (LAG, $K_m = 6$ mM) pathways in the kidney with distinct kinetic properties and expression patterns along the proximal tubule. According to these authors [59–61], the LAG system would (i) be found predominantly in the outer cortex (proximal convoluted tubule, S1 and S2 cell types), (ii) handle galactose very poorly, (iii) present high-affinity phlorizin (HAP) binding sites, and (iv) demonstrate a 1 Na^+:1 glucose stoichiometry. In contrast, the HAG system would (i) be found predominantly in the outer medulla (late proximal straight tubule, S3 cell-types), (ii) handle both glucose and galactose, (iii) present low affinity phlorizin (LAP) binding sites, and (iv) demonstrate a 2 Na^+:1 glucose stoichiometry. Since then, the latter system has been ascribed to the expression in the kidney of the SGLT1 gene [14, 40–41], a cloned entity first isolated from the rabbit (rSGLT1, [21]) and human (hSGLT1, [22]) small intestines and shown to have the kinetic characteristics expected for the HAG pathway using *in vitro* expression systems [7, 45, 65, 69]. There is some controversy, however, as to which of the three clones recently isolated from human (Hu14-hSGLT2, [25, 68]), pig (SAAT1-pSGLT2, [31, 35]), and rat (rat SGLT2 [71]) kidney cDNA libraries might in fact represent the former system: (i) sugar-evoked currents in Hu14-hSGLT2 cRNA-injected oocytes were < 1 nA [25], in contrast to those of 1000–2000 nA observed for SGLT1 and SAAT1-pSGLT2 [35]; (ii) the close relationship of Na^+-dependent nucleoside cotransport to Hu14 and the substantial evolutionary distance of Hu14 from the established SGLTs suggest that Hu14 is a nucleoside carrier [48]; (iii) the expression of SAAT1-pSGLT2 mRNA was reported to be strong in intestine, spleen, liver, and muscle but low in kidney [31], so that it has even been proposed that SAAT1-pSGLT2 be renamed SGLT3 [71]; and (iv) to our knowledge, the localization of SAAT1-pSGLT2 along the nephron has yet to be established, a quite important matter in view of the recent demonstration of SGLT activity in dog distal thick ascending limbs [67]; indeed, SAAT1-pSGLT2 was cloned from the pig kidney cell line LLC-PK_1 [31] showing functional differentiation patterns of proximal tubule cells [33, 47] but hormonal sensitivity which resembles to some extent that of the medullary thick ascending loop [24]. Still, the recent finding that patients with glucose-galactose malabsorption do not show glucosuria [58, 70] should be taken as strong evidence for molecular heterogeneity of SGLT systems in the kidney.

It would thus appear that the main question to address at this time is not whether there is more than one SGLT system in the kidney but rather whether the kinetic heterogeneity observed in BBMV isolated from the kidney cortex and/or medulla is the unique and direct consequence of this molecular diversity. Indeed, the validity of the latter equation rests on a number of assumptions that may require thorough examination. For example, in the years following Turner and Moran's studies [59–61], a number of papers appeared that also reported SGLT heterogeneity in intestinal BBMV [10, 18, 20]. However, a careful reevaluation of such studies using similar preparations from the human [38], rabbit [13], and guinea-pig [37] small intestines clearly indicated that SGLT1 is the only glucose carrier involved in these tissues, and the latter conclusion is strongly supported by the concomitant demonstration that patients with glucose-galactose malabsorption bear a single point mutation in the SGLT1-cDNA that fully accounts for the intestinal defect [58, 70]. On a theoretical point of view too, it should be appreciated that kinetic heterogeneity may also result from particular transport mechanisms relating to either monomeric [6, 18, 26, 51, 53] or oligomeric proteins [13, 29, 30]. Indeed, following the demonstration by inactivation radiation studies that the intestinal and renal SGLT proteins may form oligomeric complexes [2, 55–56, 62], a number of reports appeared [8, 19, 29–30, 66] that challenged the interpretation of Turner and Moran's results [59–61]. In agreement with such studies, Chenu and Berteloot [13] proposed a quite simple dimeric model of cotransport with mixed positive and negative cooperativities for Na^+ and glucose binding, respectively, that may fully account for the kinetic properties usually taken as evidence for the existence of two distinct SGLT transport systems: (i) upward deviations from linearity in Eadie-Hofstee plots, (ii) different Na^+:glucose stoichiometries at low and high sugar concentrations, and (iii) partial inhibition by substrate analogues and/or inhibitors. While the first two predictions of this model could not be demonstrated in the rabbit jejunum [13] and hSGLT1-cRNA injected oocytes [12], results that do not rule out, however, a polymeric structure of the SGLT1 protein [13], it has been shown since that the extent of cooperativity between subunits may be modulated through their association with RS1-type proteins which can be found in the small intestine (pig, rabbit, sheep, man) and in both the renal outer cortex and outer medulla (pig, rabbit, man) [30, 66]. Finally, the possibility that the anatomical separation achieved by

Turner and Moran [59–61] may only be apparent should also be considered. As noted by the authors themselves although never addressed, the possibility remains that the two SGLT pathways observed in their studies are, in fact, manifestations of the same transport protein in different lipid environments [59]. Moreover, it would also appear from recent studies that the regulation of SGLT1 activity is post-transcriptional since it is correlated with the protein concentration in the BBM membrane [52] but not with the amount of homologous mRNA [32]. Accordingly, the studies of Pajor et al. [44] provide molecular evidence for two SGLTs in the rabbit kidney that should be considered as indirect evidence only and they do not rule out the possibility of different post-transcriptional modifications (whether related or not to the differential expression of RS1-like polypeptides) of a unique protein in the S1/S2 as compared to the S3 segments of the proximal tubule. It thus seems fair to conclude that the ''two independent carrier hypothesis'' of Turner and Moran [59–61] is not the sole interpretation of their kinetic data and, as such, needs further reassessment.

In this paper, we thus reevaluated the kinetics of renal SGLT using rabbit renal BBMV isolated from the whole kidney cortex and a fast-sampling, rapid-filtration apparatus (FSRFA [5], US patent #5, 330, 717) for uptake measurements. It should be emphasized that no attempt was made in our studies to separate the HAG and LAG transport pathways according to regional differences along the proximal tubule on the rationale that: (i) a full separation may not be easily achieved by dissection alone, as acknowledged by Turner and Moran [59, 61] in their original studies and clearly indicated by the more recent work of Pajor et al. [44] and Silverman et al. [54], (ii) the low yield in BBMV which is expected following anatomical separation would preclude extensive kinetic studies to be performed, (iii) kinetic separation may only be apparent (*see discussion above*), and (iv) it would be possible to analyze simultaneously the kinetic characteristics of the two transport pathways with respect to a number of critical issues relating to the involvement of the SGLT1 and SGLT2 transport systems in this preparation. While our results do confirm the kinetic heterogeneity of SGLT in kidney BBMV, it is also shown that both of the HAG and LAG transport pathways demonstrate similar energies of activation (E_a) for a full catalytic cycle, accept galactose as an alternative substrate, and are inhibited competitively by phlorizin with identical K_i values. Comparisons of HAG expression in rabbit intestinal and renal BBMV, and of SGLT characteristics in renal BBMV *vs.* cRNA-injected oocytes expressing the cloned SGLT1 and SGLT2 systems lead us to conclude that the kinetic heterogeneity observed in our studies most likely reflects different transport properties of rSGLT1 rather than coexpression of distinct rSGLT1 and rSGLT2 proteins.

Materials and Methods

Materials

Rabbits were purchased from the Maple Lane Farm (Clifford, Ontario) or the ''Ferme de Sélection Cunipur'' (St-Valérien, Québec). D-[1-^{3}H(N)]-glucose (specific activity 10–15 Ci/mmol) was supplied by New England Nuclear (NEN), the BCA (bicinchoninic acid) protein assay kit by Pierce, unlabeled D-glucose by Sigma, phlorizin and ultrapure salts by Aldrich, and amiloride hydrochloride and scintillation cocktail (β-blend) by ICN Biomedicals. Cellulose nitrate filters (12.5 mm diameter, 0.65 μm pore size) were obtained from Micro Filtration Systems (MFS). All other chemicals were of the highest purity available.

Preparation of Brush Border Membrane Vesicles

Large batches of renal BBMV were prepared from the whole kidney cortex of male, 2.0–2.5 kg New-Zealand white rabbits essentially as described previously for the rabbit jejunum [3, 13, 36]. Briefly, cortex slices were introduced into the homogenate media (18 mM HEPES-Tris buffer pH 7.0 containing 1 mM EDTA and 250 mM sucrose) at a 1:20 ratio (w:v), and homogenized at 4°C in a Waring blender for 1 min at full speed. BBM were precipitated by addition of 10 mM $MgCl_2$ [13, 36], purified in a P_2 fraction [3], and resuspended in a minimal volume of 50 mM HEPES-Tris buffer (pH 7.0) containing 300 mM mannitol and 0.1 mM $MgSO_4$ [13]. The P_2 fractions were divided into 500 μl aliquots and frozen in liquid N_2 [13, 36]. On the day of use, a suitable number of aliquots of frozen P_2 were thawed and diluted at a 1:10 ratio (w:v) in the resuspension buffer (50 mM HEPES-Tris buffer (pH 7.0) containing 0.1 mM $MgSO_4$, 300 mM mannitol, and 200 mM KI) to which was added 3 μM valinomycin to ensure full equilibration of the cation [13, 36]. BBMV were prepared as a final P_4 pellet [3] and resuspended in the valinomycin-free resuspension buffer at a protein concentration of 28–35 mg/ml [13]. To ensure stability of the preparation over the course of the experiment, 25 μl aliquots of BBMV were frozen in liquid N_2 until the time of assay [13, 36].

Uptake Assays

Initial rates of Na^+-dependent, ^{3}H-D-glucose uptake were determined under zero-trans gradient conditions of both ion and substrate using the automated FSRFA developed in our laboratory [5]. For each assay, 20 μl of BBMV were thawed, prewarmed, and loaded into the apparatus. Uptake was initiated by injecting the vesicles into 480 μl of 50 mM HEPES-Tris buffer (pH 7.0) containing (in mM): 0.1 $MgSO_4$, 0.5 amiloride, 300 mannitol, 50 KI, 150 of either NaI or choline iodide for Na^+-gradient or Na^+-free conditions, respectively, and 4 μM tracer D-glucose or galactose. For kinetic parameter determinations, 12 concentrations of cold D-glucose or galactose were used (0, 0.01, 0.025, 0.05, 0.1, 0.25, 0.5, 1, 2, 5, 10, and 200 mM) and osmolarity was kept constant by varying mannitol concentrations to satisfy a total concentration of cold substrate + mannitol of 300 mM. For phlorizin inhibition studies, the uptake media also contained 0.5, 1, 5, 10, 30, and 50 μM of the SGLT inhibitor. Uptakes were performed in the thermostated chamber of the FSRFA [5] and determined by a 9-point automatic sequential sampling of the uptake mixture at 1-sec intervals [13]. At each time point, 50 μl of the uptake mixture was injected into 1 ml of ice-cold stop solution (50 mM HEPES-Tris buffer (pH 7.0) containing (in mM): 0.1 $MgSO_4$, 300 mannitol, 1 phlorizin, and 200 of either NaCl or choline chloride for Na^+-gradient or Na^+-free conditions, respec-

tively). The stopped mixture was then filtered through 0.65 μM cellulose nitrate filters, and the filters were washed three times with 1 ml of ice-cold stop solution [5, 13]. The substrate content of the vesicles was then determined by liquid scintillation counting as described previously [13].

Under the conditions of our uptake assays, the initial rates of 50 μM D-glucose uptake were linear with protein concentrations over the range 1–35 mg protein/ml [13]. Protein was measured with the BCA assay kit using bovine serum albumin as a standard.

Data Analysis

Four (phlorizin inhibition studies) or five (all other studies) uptake time courses were run at each of the substrate concentrations used in the respective experiments. Initial rates of tracer transport (v_i^*, $pmol \cdot sec^{-1} \cdot mg^{-1}$ protein) were determined over the 1–7-sec time course of the assays by linear (15–25°C) or polynomial (30°C) regression analysis as justified previously [13]. The kinetic parameters of glucose and galactose transport were estimated by nonlinear regression analysis of the initial rate data, thus assuming that the added cold substrate acts as an ideal competitive inhibitor of tracer transport [6, 13, 38]. The equations used corresponded to either one or two Michaelis-Menten components working in parallel with passive diffusion (referred to in the following as the one-site or the two-sites models, respectively) and have been both justified and given in full in a previous paper from our group, as well as the strategy aimed at model discrimination [13]. The best model fit to the data is reported in each of the figures, and an Eadie-Hofstee transformation of the carrier-mediated process is also presented where appropriate for visual appraisal of the goodness of fit [6, 13, 38]. Linear and nonlinear regression analyses were performed using a commercial software (Enzfitter, R.J. Leatherbarrow, copyright 1987, Elsevier-Biosoft). Since both of the robust and explicit weighting routines of this software were used for data analysis, the errors associated with v_i^* determinations and kinetic parameter values reported in this paper represent the standard errors of regression (SER) on these parameters. When shown, the evaluation of the 95% confidence intervals was performed using the commercial software ''P.Fit'' (copyright 1990 Fig.P Software, Biosoft).

Results

Heterogeneity of SGLT in Renal BBMV

The dependence of the initial rates of tracer D-glucose (4 μM) transport upon increasing cold substrate concentrations is shown in Fig. 1 for two similar experiments performed at 20°C using different batches of BBMV and cold glucose concentrations. In both experiments, the initial rate data were best described by the two-sites model equation, and the kinetic parameter values corresponding to the HAG and LAG transport pathways are given in Table 1. The reproducibility of our kinetic approach appears very good, as also clearly demonstrated in Fig. 1 where it can be appreciated that the two fits are not significantly different from each other at the 95% confidence level. The uptake time courses generated at each of the glucose concentrations tested in the two independent experiments were thus pooled to determine a unique set of initial rates of tracer uptake. The kinetic

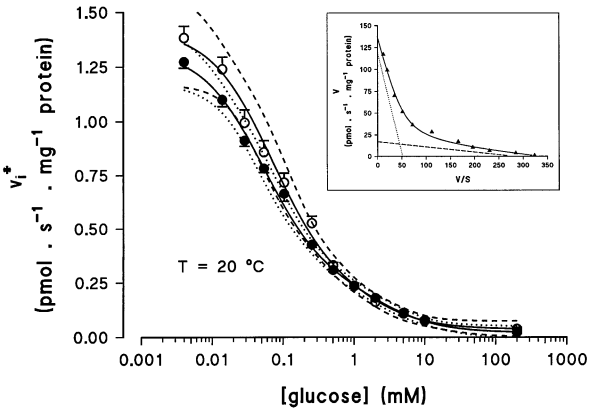

Fig. 1. SGLT heterogeneity in renal BBMV at 20°C. BBMV were resuspended in 50 mM HEPES-Tris buffer (pH 7.0) containing 0.1 mM $MgSO_4$, 300 mM mannitol, and 200 mM KI. The uptake medium contained (final concentrations): 50 mM HEPES-Tris buffer (pH 7.0), 0.1 mM $MgSO_4$, 0.5 mM amiloride, 100 mM mannitol, 50 mM KI, 150 mM NaI, 4 μM D-(^{3}H)glucose, and 0–200 mM glucose. Osmolarity was kept constant by varying mannitol concentrations to satisfy a total concentration of glucose + mannitol of 200 mM. Values shown are the mean initial rates ±SER determined from five uptake time courses recorded at each substrate concentration as described in the text. (○) and (●) represent two independent experiments. Missing error bars were smaller than the symbol size. The full lines shown are the best-fit curves corresponding to the two-sites model, and the broken lines represent the 95% confidence interval of the regressions. All kinetic parameters are given in Table 1. Inset: Eadie-Hofstee plot of the carrier-mediated component of SGLT constructed from the nonlinear regression analysis of the pooled data with kinetic parameters as given in Table 1. Broken lines represent the individual contribution of the HAG and LAG transport pathways to total transport. Error bars were voluntarily omitted for clarity of the figure.

heterogeneity of SGLT in rabbit renal BBMV purified from the whole kidney cortex is best emphasized by the Eadie-Hofstee transformation of the pooled data (inset of Fig. 1 with kinetic parameters as given in Table 1).

Transport Heterogeneity and Na^+-independent Glucose Transport

The possibility that glucose transport in renal BBMV might occur in the complete absence of Na^+ [11, 23] was evaluated by comparing: (i) tracer D-glucose uptake (4 μM) in the presence of 150 mM Na^+ and 200 mM cold glucose, experimental conditions which should give, according to the kinetic parameter values of Table 1, a reliable estimate of the diffusional component of transport, and (ii) tracer D-glucose uptake (4 μM) in the presence of 150 mM choline substituted for Na^+, experimental conditions that provide, as clearly indicated by the displacement curve in Fig. 1, the highest sensitivity for measuring any carrier-mediated transport. As illustrated in Fig. 2, the uptake data under conditions (i) and (ii)

Table 1. Kinetic parameters of SGLT transport at 20°C in rabbit renal BBMV isolated from the whole kidney cortex

Kinetic parameters	Experiment 1	Experiment 2	Pooled data
V_{max1} (pmol. sec^{-1} mg^{-1} protein)	14.7 ± 1.5	20.5 ± 4.0	17.1 ± 2.4
K_{ml} (μM)	54 ± 6	68 ± 12	60 ± 8
V_{max2} (pmol. sec^{-1} mg^{-1} protein)	147 ± 21	95 ± 23	119 ± 22
K_{m2} (mM)	2.7 ± 0.5	2.0 ± 0.8	2.3 ± 0.6
k_D (pmol. sec^{-1} mg^{-1} protein. mM^{-1})	5.3 ± 1.4	9.2 ± 1.7	7.7 ± 1.6

Values shown were determined from the data presented in Fig. 1.

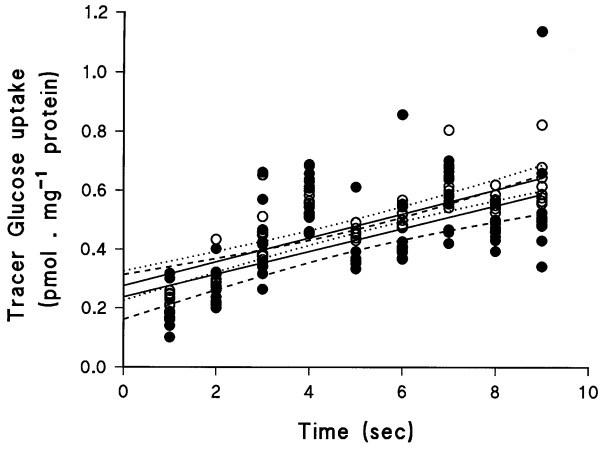

Fig. 2. Transport heterogeneity and Na^+-independent glucose transport. BBMV were resuspended as described in the legend to Fig. 1. The uptake media contained (final concentrations): 50 mM HEPES-Tris buffer (pH 7.0), 0.1 mM $MgSO_4$, 0.5 mM amiloride, 50 mM KI, 4.24 μM D-(^{3}H) glucose, and either 100 mM mannitol, 200 mM glucose and 150 mM NaI (●) or 300 mM mannitol and 150 mM choline iodide (○). Ten uptake time courses were recorded at 20°C under each of these experimental conditions. The linear regression lines ($y = a \cdot t + b$) shown are the best-fit lines over all individual data points in each experiment. Regression parameters: a (pmol · sec^{-1} · mg^{-1} protein), 0.0356 ± 0.0045 (●), 0.0423 ± 0.0030 (○); and b (pmol · mg^{-1} protein), 0.236 ± 0.026 (●), 0.257 ± 0.017 (○).

were not significantly different from each other at the 95% confidence level, thus clearly demonstrating that Na^+ is mandatory for glucose transport through the HAG and LAG pathways, and that Na^+-independent transport does not contribute in any way to SGLT heterogeneity. Moreover, the mean slope value of 0.039 ± 0.003 pmol · sec^{-1} · mg^{-1} protein estimated for the pooled data in Fig. 2 is equivalent to a k_D value of 9.20 ± 0.07 pmol · sec^{-1} · mg^{-1} protein. mM^{-1} in these experiments, in agreement with the data in Table 1 at 20°C.

Heterogeneity of Na^+-D-Galactose Cotransport in Renal BBMV

Hu14 [68], a human cDNA claimed to represent hSGLT2 [25], and SAAT1, a cDNA cloned from LLC-PK_1 cells [31] and later proposed to represent pSGLT2 [35], were reported not to transport or to transport very weakly D-galactose, respectively, when expressed in *Xenopus laevis* oocytes. As shown in Fig. 3, however, heterogeneity of both D-glucose and D-galactose transport could be readily observed at 25°C in our renal BBMV preparations. Moreover, Table 2 indicates that high and low affinity galactose transport occurred with V_{max} values similar to those of HAG and LAG transport, thus showing that the two substrates do share the two transport pathways. Interestingly too, galactose was transported with lower affinity than glucose through both pathways; however, the K_m for galactose relative to glucose transport through the HAG and LAG routes were increased by 3.9- and 7.8-fold, respectively.

Phlorizin Inhibition of SGLT in Renal BBMV

Based on phlorizin inhibition studies of SGLT in rabbit renal BBMV isolated from the outer cortex and outer medulla, it has been reported that the HAP and LAP binding sites correspond to the LAG and HAG transport pathways, respectively [61]. In agreement with Turner and Moran's studies [61], an IC_{50} value ≈ 1 μM was estimated for phlorizin inhibition of α-methylglucose (AMG) transport through Hu14/hSGLT2 [25] (this value is equivalent to $K_i \approx 0.4$ μM when assuming competitive inhibition and considering both the AMG concentration of 2 mM used and the K_m value of 1.6 mM for AMG transport reported in the studies of Kanai et al. [25]). In contrast, K_i values of 16–18 μM (at holding membrane potentials V_m of -110 to -50 mV) or ≈ 37 μM (at V_m = −10 mV) were determined for phlorizin inhibition of

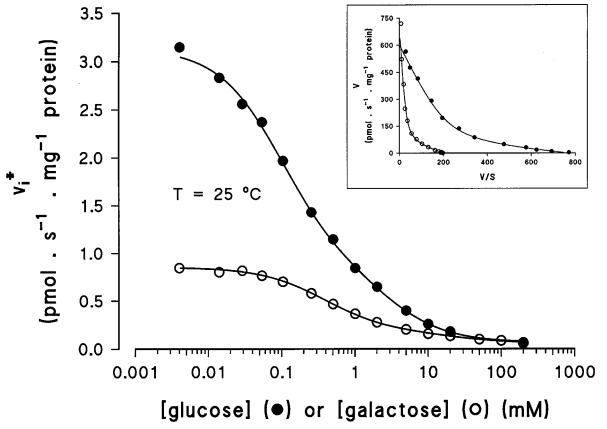

Fig. 3. Heterogeneity of Na^+-D-galactose cotransport in renal BBMV at 25°C. Experimental conditions were as described in the legend to Fig. 1 (●) or galactose was substituted for glucose in the uptake media (○). Values shown are the mean initial rates ±SER determined from five uptake time courses recorded at each substrate concentration as described in the text. Error bars were smaller than the symbol size. Lines shown are the best-fit curves corresponding to the two-sites model. All kinetic parameters are given in Table 2. *Inset:* Eadie-Hofstee plot of the carrier-mediated components of glucose (●) and galactose (○) transport.

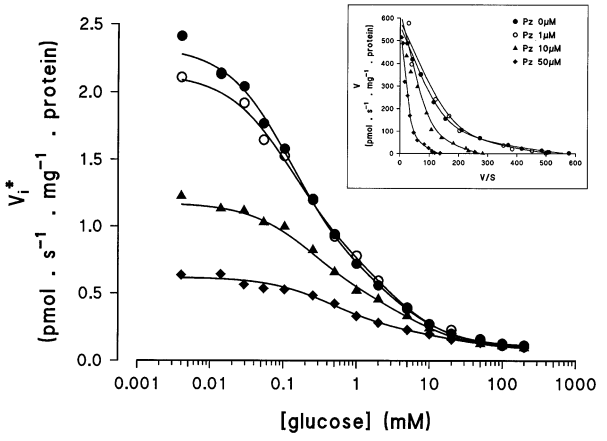

Fig. 4. Phlorizin inhibition of SGLT in renal BBMV at 25°C. Experimental conditions were as described in the legend to Fig. 1 except that phlorizin concentrations of 0 (●), 1 (○), 10 (▲), and 50 (♦) μM were added to the uptake media. Values shown are the mean initial rates ±SER determined from four uptake time courses recorded at each substrate concentration as described in the text. Error bars were smaller than the symbol size. Lines shown are the best-fit curves corresponding to the two-sites model. All kinetic parameters are given in Table 3. Inset: Eadie-Hofstee plot of the carrier-mediated component of SGLT.

Table 2. Kinetic parameters of glucose and galactose transport at 25°C in rabbit renal BBMV isolated from the whole kidney cortex

Kinetic parameters	Substrate	
	Glucose	Galactose
V_{max1} (pmol. sec^{-1} mg^{-1} protein)	56 ± 7	65 ± 4
K_{ml} (μM)	99 ± 11	384 ± 16
V_2 (pmol. sec^{-1} mg^{-1} protein)	546 ± 49	633 ± 95
K_{m2} (mM)	2.7 ± 0.5	21.1 ± 4.9
k_D (pmol. sec^{-1} mg^{-1} protein. mM^{-1})	16.7 ± 4.2	14.5 ± 2.7

Values shown were determined from the data presented in Fig. 3.

AMG transport through pSGLT2 [35], and these values thus appear higher than the K_i values of 6–10 μM estimated for rSGLT1 [7, 65, 69].

This question was thus reevaluated in our rabbit renal BBMV preparations by repeating at 25°C the experiments of Fig. 1 for different concentrations of phlorizin. The initial rate data were best-fitted to the two-sites model equation as shown in Fig. 4 for representative concentrations of phlorizin, and the corresponding kinetic parameter values are given in Table 3. Figure 5 clearly indicates that the V_{max} of both HAG and LAG transport were unaffected by phlorizin, thus demonstrating that phlorizin inhibits competitively the two transport pathways (it should be noted that the mean V_{max1} and V_{max2} values of 41 ± 6 and 524 ± 49 pmol · sec^{-1} · mg^{-1} protein, respectively, compare fairly well to those determined in Table 2 for a different membrane preparation). Therefore, the apparent Michaelis constants (K_a) in Table 3 were fitted to Equation (1) in which K_m and K_i have their usual meanings.

$$K_a = K_m \cdot \left[1 + \frac{(I)}{K_i}\right] \quad (1)$$

These results are shown in Fig. 6 from which K_{m1} and K_{m2} values of 0.113 ± 0.007 and 3.3 ± 0.2 mM could be estimated for HAG and LAG transport, respectively, in agreement with the results of Table 2. Interestingly, however, similar K_i values of 15.3 ± 3.0 and 14.5 ± 2.2 μM were observed for phlorizin inhibition of the two SGLT pathways.

Temperature Effects

The temperature dependence of SGLT has been analyzed in rat [27], hog [17] and rabbit [28] renal BBMV. Nonlinear Arrhenius plots were found showing either a transition temperature at 15°C [17, 27] or curvilinearity [28] over the whole range of temperatures. Since these early studies did not resolve the HAG and LAG transport pathways, such nonlinear plots are compatible with SGLT heterogeneity in renal BBMV, as also inferred from the

Table 3. Effects of phlorizin on the kinetic parameters of SGLT transport at 25°C in rabbit renal BBMV isolated from the whole kidney cortex

Kinetic parameters	[Phlorizin] (μM)						
	0	0.5	1	5	10	30	50
V_{max1} (pmol. sec^{-1} mg^{-1} protein)	51 ± 9	42 ± 9	42 ± 10	33 ± 10	42 ± 10	36 ± 15	44 ± 12
K_{a1} (μM)	119 ± 19	130 ± 26	120 ± 28	122 ± 33	234 ± 44	390 ± 130	447 ± 102
V_{max2} (pmol. sec^{-1} mg^{-1} protein)	515 ± 49	433 ± 43	545 ± 45	556 ± 134	586 ± 57	503 ± 57	528 ± 89
K_{a2} (mM)	3.6 ± 0.7	3.6 ± 0.7	3.2 ± 0.6	4.5 ± 1.5	6.1 ± 1.1	9.1 ± 2.4	15.6 ± 5.4
k_D (pmol. sec^{-1} mg^{-1} protein. mM^{-1})	25.7 ± 1.3	24.3 ± 1.4	23.8 ± 1.3	34.0 ± 4.8	20.7 ± 1.0	21.8 ± 1.2	23.4 ± 1.8

Values shown were determined from the data presented in Fig. 4.

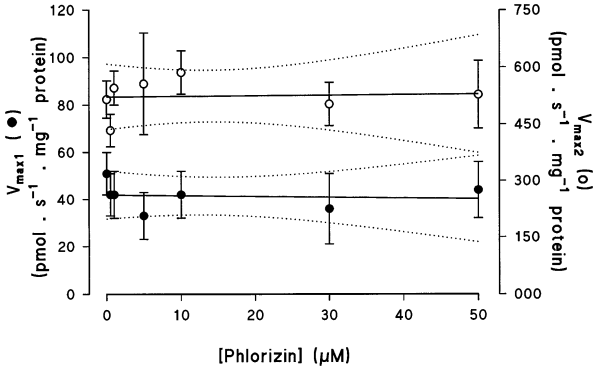

Fig. 5. Mechanism of SGLT inhibition by phlorizin. The kinetic parameters V_{max} given in Table 3 were plotted against phlorizin concentrations. The linear regression lines and 95% confidence intervals shown demonstrate that phlorizin has no effect on the V_{max} of the HAG (●) and LAG (○) transport pathways, thus indicating the competitive nature of transport inhibition through both pathways.

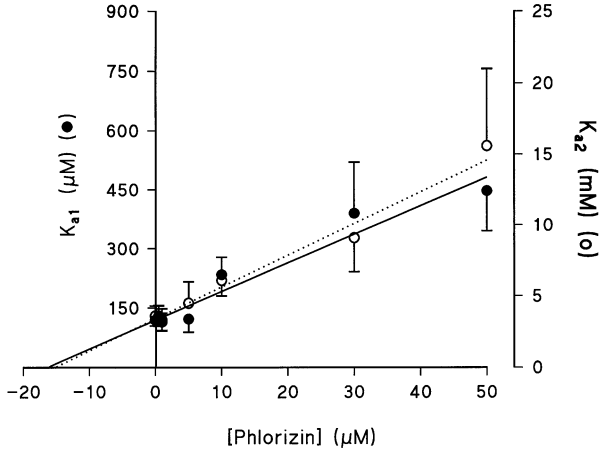

Fig. 6. K_i determination of SGLT inhibition by phlorizin. The kinetic parameters K_m given in Table 3 were plotted against phlorizin concentrations. The linear regression lines shown are the best-fit lines corresponding to Equation (1) in the text, and the identical intercepts of these lines on the x axis demonstrate that the HAG (●, full line) and LAG (○, dotted line) transport pathways are inhibited with equal potency by phlorizin. Estimated K_i values are given in the text.

studies of Brot-Laroche et al. [10] in guinea-pig intestinal BBMV where a LAG transport pathway seemed to be activated at higher temperatures.

This hypothesis was tested in our renal BBMV preparations as follows. Experiments similar to those of Fig. 1 were repeated at 15 and 30°C. The kinetic data at these two temperatures could be best resolved when assuming a two-sites model with kinetic parameters as given in Table 4. It was then possible to construct the Arrhenius plots pertaining to the kinetic parameters determined in Tables 1–4 (Fig. 7) from which the following observations can be made: (i) linear plots are obtained over the 15–30°C range of temperatures for all kinetic parameters, although the K_m of the LAG transport pathway proves to be quite insensitive to temperature (mean value = 2.9 ± 0.5 mM, Fig. 7*B*, open circles); (ii) similar E_a values can be determined from the V_{max} data pertaining to the HAG and LAG transport pathways (E_a = 45.0 ± 3.1 and 40.2 ± 2.2 kcal · K^{-1} · mol^{-1} for HAG and LAG, respectively, Fig. 7*A*); and (iii) an E_a value of 25.7 ± 2.1 kcal · K^{-1} · mol^{-1} can be estimated from the K_m data relative to HAG transport (Fig. 7*B*, closed circles) which falls within the range of E_a = 18.0 ± 3.4 kcal · K^{-1} · mol^{-1} that can be calculated for passive diffusion of glucose (Fig. 7*B*, open triangles).

Discussion

General Comments

In this paper, the kinetics of SGLT were reevaluated in rabbit renal BBMV isolated from the whole kidney cor-

Table 4. Kinetic parameters of SGLT transport at 15 and 30°C in rabbit renal BBMV isolated from the whole kidney cortex

Kinetic parameters	Temperature	
	15°C	30°C
V_{max1} (pmol. sec^{-1} mg^{-1} protein)	4.1 ± 0.3	365 ± 87
K_{m1} (μM)	29 ± 3	311 ± 38
V_{max2} (pmol. sec^{-1} mg^{-1} protein)	49 ± 10	1457 ± 139
K_{m2} (mM)	3.2 ± 0.8	3.1 ± 1.1
k_D (pmol. sec^{-1} mg^{-1} protein. mM^{-1})	3.6 ± 0.4	17.8 ± 1.3

Experimental conditions were as described in the legend to Fig.1, and kinetic parameters were estimated by nonlinear regression analysis as indicated in the text.

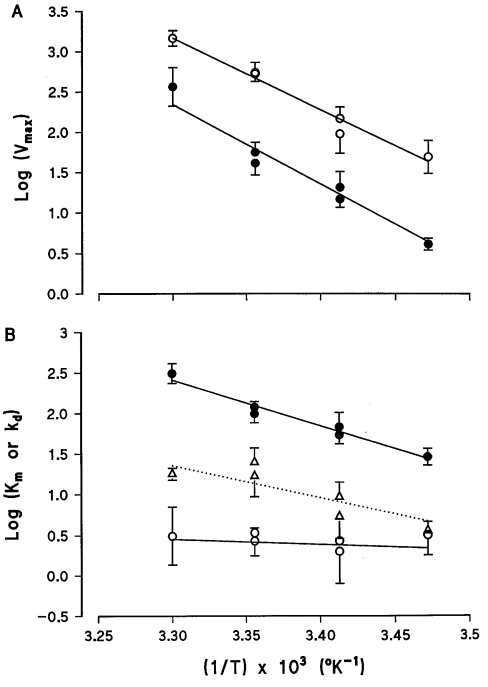

Fig. 7. Temperature effects on glucose transport through the HAG (●), LAG (○), and diffusional (△) pathways in renal BBMV. Arrhenius plots were constructed for the V_{max} (*A*), and K_m and k_D (*B*) values given in Tables 1–4. The slope of the linear regression lines shown allow the calculation of the energies of activation (E_a) given in the text (slope = $-E_a/2.3 \cdot R$).

tex, and it should be emphasized first that our kinetic experiments: (i) involved a dynamic approach [6, 18] in which the true initial rates of transport were determined from 4 to 5 uptake time courses recorded under all experimental conditions with a FSRFA [5, 13, 38], (ii) evaluated the kinetic parameters of transport by weighted, nonlinear regression analysis of the initial rate data relative to tracer concentration that precludes undue transformations of the experimental data and avoids a number of complications associated with it [5, 6, 13, 38], and (iii) paid particular attention to the stability of the vesicle preparation [36] and to the control of temperature, pH, osmolarity, ionic strength, and membrane potential which was clamped to 0 mV using iodide as a highly permeant anion [4]. From the results of Fig. 1 and Table 1 at 20°C, and Tables 2–3 at 25°C, it can be concluded that the use of BBMV prepared from the same large batch of P_2 fractions minimizes animal-to-animal variations of uptake data and that our experimental conditions ensure high reproducibility of the results. Therefore, meaningful comparisons can be made between experiments without costly and time-consuming data replication.

It is important to emphasize next that SGLT heterogeneity was observed in rabbit kidney BBMV under experimental conditions that failed to reveal similar heterogeneity in equivalent preparations from the rabbit [13] and human [38] jejunum. The present studies thus validate further our kinetic approach aimed at resolving multicomponent transport systems [6, 13, 38] and confirm those of Turner and Moran [59] showing that the initial rate data in the whole kidney cortex is compatible with the presence of both HAG and LAG transport pathways. Still, the K_m values reported in Tables 1 (20°C) and 4 (15°C) appear lower than those of 0.35 and 6.0 mM previously estimated at 17°C in a similar preparation for HAG and LAG transport, respectively [59]. This apparent discrepancy can be easily resolved from the consideration that Turner and Moran's data [59] were obtained at a 40 mM Na^+ concentration rather than the saturating Na^+ concentration of the 150 mM used throughout our experiments [60, 61].

SGLT Expression in Rabbit Renal and Intestinal BBMV

Because a cDNA clone with full identity to intestinal rSGLT1 has been isolated from the rabbit kidney cortex [40], it can be assumed, as also done by a number of authors [25, 30, 35, 44, 54, 71], that the HAG pathway should represent the functional expression of the SGLT1 protein in this tissue. In this respect, Na^+ was found to be an essential activator of SGLT in the rabbit kidney (Fig. 2), a property clearly demonstrated for rSGLT1 in the small intestine [13]. Still, under symmetrical conditions (20°C, 0 mV, and 150 mM Na^+ gradient), the K_m value of HAG transport is some 2.3- ± 0.4-fold lower in the former as compared to the latter tissue (60 ± 8 μM in Table 1 *vs.* 139 ± 5 μM in [13], respectively). It can thus be concluded that this highly significant difference should reflect how rSGLT1 is expressed functionally in

renal as compared to intestinal BBMV. Interestingly, a similar difference is seen in man for HAG transport in the jejunum (K_m = 0.6–0.9 mM in [38]) and the kidney ($K_m \approx 0.3$ mM in [63]). Therefore, these data point to the fact that the same SGLT1 gene leads to differential expression of the SGLT1 protein in the two tissues.

One is thus led to question whether rSGLT1 activity is modulated by the lipid composition and/or the physical state of the membrane. A conclusive answer to this question may not be given at this time. However, the following pieces of evidence point out to a minor role of this two elements in affecting SGLT1 activity: (i) it is quite remarkable that similar K_m values have been reported for SGLT1 expression in intestinal BBMV (*see* values reported above) and oocytes injected with rSGLT1-cRNA (100–200 [45] and 117–126 [66] μM) or hSGLT1-cRNA (0.8 [34] and 1.2 [12] mM); (ii) the temperature studies of Fig. 7 show linear Arrhenius plots for the V_{max} (E_a = 45.0 ± 3.1 kcal $\cdot K^{-1} \cdot$ mol^{-1}) and K_m (25.7 ± 2.1 kcal $\cdot K^{-1} \cdot$ mol^{-1}) data regarding glucose transport through the renal HAG pathway; and (iii) if one also assumes linearity in the Arrhenius plots of intestinal SGLT1 between 20 and 35°C, quite similar E_a values of 32.7 and 15.8 kcal $\cdot$ K$^{-1} \cdot$ mol^{-1} can be calculated from our previous studies in rabbit jejunal BBMV [13] for the V_{max} and K_m data, respectively. Indeed, our conclusion contrasts with that of previous studies in which: (i) the Arrhenius plots were constructed from the initial rate data estimated at one substrate concentration only [9, 17, 27–28], and (ii) the renal HAG and LAG pathways were not resolved [17, 27–28]. Because initial rate equations of transport mechanisms are complex functions of both microscopic constants and substrate concentrations, and since different rate-limiting steps may govern transport activity at different temperatures, linear Arrhenius plots are not usually expected under these conditions, even when considering the simplest case of a unique transport protein. Therefore, the E_a values of 45.0 ± 3.1 kcal $\cdot K^{-1} \cdot$ mol^{-1} determined in our studies from the V_{max} data (Fig. 7*A*) may only be compared to those of 17.4–21.0 kcal $\cdot K^{-1} \cdot$ mol^{-1} calculated from the Q_{10} values of Parent et al. [46] pertaining to the V_{max} of rSGLT1 in cRNA-injected oocytes. In contrast also to the studies of Parent et al. [46], the K_m of HAG transport in renal BBMV shows a strong temperature dependence (Fig. 7*B*). The reason for these differences is not obvious at this time but for the fact that such experiments are more difficult to perform in oocytes studies [46].

The conclusion above that the lipid composition and/or the physical state of the membrane do not affect much the functioning of rSGLT1 would suggest that post-transcriptional modifications of the protein may be responsible for the differential expression of rSGLT1 in the small intestine and the kidney, in agreement with recent studies showing that the regulation of SGLT1 activity is correlated with the protein concentration in the BBM membrane [52] but not with the amount of homologous mRNA [32]. The nature of this modification cannot be assessed at this time. Still, the decrease in the K_m value associated with rSGLT1 (HAG) expression in the kidney (60 ± 8 μM, Table 1), and the apparition of a LAG pathway in this tissue (K_m = 2.9 ± 0.5 mM, mean of the six experiments performed at different temperatures), are features which are indeed reminiscent of those reported by Veyhl et al. [66] upon coinjection of RS1 with rSGLT1 into *Xenopus* oocytes: under these conditions, the K_m of rSGLT1 decreased from 117–126 to 17–29 μM and a low-affinity pathway with K_m value of 0.9–1.9 mM appeared [66]. Unfortunately, however, the range of K_m values reported for SAAT1-pSGLT2 (1.7–4.0 mM in [35]), Hu14-hSGLT2 (1.6 mM in [25]), and rat SGLT2 (3 mM in [71]) in cRNA-injected oocytes also encompasses that determined for the LAG pathway in the above studies.

Kinetic Characteristics of the Renal LAG Pathway

Following Turner and Moran's hypothesis [59–61] in which the renal HAG and LAG pathways would represent distinct transport systems, the latter has been ascribed to the expression of a SGLT2 protein [25, 35, 71] that has yet to be cloned in the rabbit. However, this simple equation ignores the following facts: (i) a number of inactivation radiation studies agree that the intestinal and renal SGLT proteins may form oligomeric complexes [2, 55–56, 62]; (ii) a number of reports appeared [8, 19, 29–30, 66] that challenge the interpretation of Turner and Moran's results [59–61]; (iii) Chenu and Berteloot [13] proposed a quite simple dimeric model of cotransport that may fully account for the kinetic properties usually taken as evidence for the existence of two distinct SGLT transport systems; and (iv) in agreement with this model, it was suggested that the extent of cooperativity between subunits might be modulated through their association with RS1-type proteins [30, 66]. Moreover, as discussed in the Introduction, there is some controversy in the literature as to which of the three clones recently isolated from kidney libraries [31, 68, 71] might in fact qualify to represent SGLT2 activity [25, 35, 71]. The question arises, then, as to what extent could the kinetic heterogeneity observed in BBMV isolated from the kidney cortex and/or medulla be the sole consequence of the proposed molecular diversity and, as discussed in details below, our studies do point out a number of inconsistencies with regard to this hypothesis.

Galactose Transport Studies

It was reported by Turner and Moran [59] that galactose is a poor inhibitor of glucose transport through LAG as

compared to HAG, and K_i values of 54–77 and 2.0–2.6 mM (ratio of 27–30-fold) can be estimated from the data of Table 2 in [59] for the former and the latter pathways, respectively. Similarly, Roigaard-Petersen et al. [49] separated low (outer cortex, $K_m \approx 15$ mM) and high (outer medulla, $K_m = 0.15$ mM) affinity galactose transport pathways (ratio of 100-fold) in the rabbit kidney. Qualitatively at least, then, our results agree with these previous studies (ratio of 55-fold, *see* Table 2) and bring further evidence, from the similar V_{max} values of glucose and galactose transport through both of the HAG and LAG pathways (Table 2), that the two substrates do share the same transport routes. Moreover, in contrast to the finding of preferential glucose uptake through LAG only [49] and through SAAT1-pSGLT2 [35] as compared to rSGLT1 [7], our studies clearly indicate, in agreement with those of Turner and Moran [47] in the kidney, that glucose is the preferred substrate of both intestinal rSGLT1 [13] (the K_m for galactose as compared to glucose transport was reduced 2.9-fold in these studies) and the renal HAG and LAG pathways (Table 2). These discrepancies may indeed relate to the facts that: (i) the kinetic studies of Roigaard-Petersen et al. [49] were not done under initial rate conditions, and (ii) the studies of Birnir et al. [7] did not fully resolved the K_m of glucose and galactose transport in rSGLT1-cRNA injected oocytes. Still, in the present studies, the apparent affinity of galactose *vs.* glucose transport through LAG was decreased by 7.8-fold as compared to 3.9-fold only through HAG (Table 2), and these results also agree qualitatively with those of Turner and Moran [59] (ratios of 9–13- and 6–7-fold can be estimated in outer cortex and medulla, respectively). Quite obviously, then, these results could be taken as evidence for two distinct and independent glucose transporters. However: (i) neither Hu14-hSGLT2 [25] nor rat SGLT2 [71] seems to transport galactose to any significant extent, and (ii) SAAT1-pSGLT2 [35] was reported to transport galactose with very low affinity ($K_m > 20$ mM); however, a more realistic K_m value of 385 mM would account for the data of Fig. 1 in [35] as can be calculated from the current values and kinetic parameters of sugar transport given in the text[2] [35]. Accordingly, there is a major difference in the galactose transport characteristics between the putative SGLT2s and the rabbit renal LAG pathway that might eventually be accounted for by species differences. Still, the available evidence also suggests that galactose transport is a distinctive property of the SGLT1 protein, so that our kidney results are also compatible with the concept that HAG and LAG transport might represent two different transport modes through the same rSGLT1 protein. In the dimeric model of Chenu and Berteloot [13], a possible interpretation would be that a higher negative cooperativity is associated with galactose as compared to glucose binding to a second substrate site (subunit). Indeed, the rate of the conformational change induced upon binding of the first substrate molecule to the transporter might be linked to the structure of a pyranose ring.

Phlorizin Inhibition Studies

It should be emphasized first that our studies appear as the most complete ones to date that ever tried to determine simultaneously the inhibitory effect of phlorizin on HAG and LAG transport pathways in BBMV isolated from the whole kidney cortex. Our results confirm beyond any doubt that phlorizin inhibits competitively renal SGLT through both pathways (Fig. 5) and demonstrate, quite unexpectedly in fact, that phlorizin is equally potent at inhibiting the two glucose transport routes (Fig. 6). One is thus led to question the experimental evidence which served to establish the notion that the rabbit kidney HAG and LAG pathways should show differential inhibition by phlorizin.

It turns out that Turner and Moran [59] concluded first that phlorizin is less effective in inhibiting D-glucose flux in outer medullary vesicles than in the outer cortical preparation when looking at phlorizin inhibition of glucose transport in the two BBMV populations. This conclusion does not seem to be justified, however, because their data of Table 2 in [59] merely report on phlorizin inhibition at a fixed glucose concentration of 1 mM. Accordingly, from the relative inhibition values reported in that Table (60 mM NaCl inward gradient at 17°C) and the kinetic parameters of glucose transport given in [59], K_i values of 7.5–11 and 5.4–15 μM can be calculated at 10–100 μM phlorizin for the outer cortical and outer medullary tissues, respectively. Interestingly, these values are not that different from ours (15 μM, Fig. 6) and could well have been taken as evidence for similar sensitivities of the HAG and LAG transport systems relative to phlorizin inhibition.

In further studies performed under equilibrium ex-

[2] At a holding potential of −50 mV, the K_m of α-methylglucose transport is 1.7 mM and a substrate concentration of 20 mM induced a current of 560 nA [35]. An I_{max} value of 608 nA can thus be calculated from the Michaelis-Menten Equation (2)

$$\frac{I_{max} * 20}{1.7 + 20} = 560 \qquad (2)$$

In the same occyte and at the same holding potential, 20 mM galactose induced a current of 30 nA, so that a K_m of 385 mM can be estimated for galactose transport from the Michaelis-Menten Equation (3)

$$\frac{608 * 20}{K_m + 20} = 30 \qquad (3)$$

change conditions (60 mM NaCl and 1 mM glucose), Turner and Moran [61] were able to resolve consistent K_d (1.48 μM) and K_i (1.36 μM) values for phlorizin binding and phlorizin inhibition of glucose transport in the outer cortex but failed to do so in the outer medulla. Still, because a low affinity binding component (K_d = 102 μM at 37°C and 60 mM NaCl equilibrated across the BBMV) could be observed in BBMV isolated from the latter tissue, and because a $K_{0.5}$ value of 51 μM was determined for phlorizin inhibition of 1 mM glucose transport under equilibrium exchange conditions (20°C and 60 mM NaCl) in this preparation, it was concluded that HAG transport should be associated with LAP binding. These two data sets are internally inconsistent, however: (i) a $K_{0.5}$ value higher than the K_d value would have been expected in the equilibrium exchange experiments (and the more so since a K_d value higher than 100 μM would be likely upon decreasing the temperature from 37 to 17°C); and (ii) the $K_{0.5}$ value does not tell much about the K_i and/or K_d values in the absence of K_m value for glucose transport (for example, the $K_{0.5}$ value of 51 μM is fully compatible under the conditions of those experiments with a K_d and/or K_i value of 15 μM for an associated K_m value of 0.4 mM as reported for HAG by Turner and Moran [59, 61]). Moreover, in the LLC-PK_1 cell line which seems to express SGLT1 almost exclusively [41], Moran et al. [39] reported K_d values of phlorizin binding at 37°C that increase from 0.2 to 2.5 μM for Na^+ concentrations decreasing from 500 to 100 mM. Similarly in the dog [54], K_i values of ≈ 0.9 μM were reported for phlorizin inhibition of SGLT under Na^+-gradient conditions (150 mM NaSCN, 25°C) in both of the outer cortical and outer medullary tissues. However, these results contrast with the phlorizin binding studies of Turner and Silverman [64] in the same species in which both HAP (K_d ≈ 1 μM) and LAP (K_d = 26 μM) sites were found in the whole kidney cortex (100 mM NaCl equilibrated across the BBMV, 37°C).

It thus seems fair to conclude that the situation is far from clear at this time, so that further insights to resolve those questions should come from the comparison of transport inhibition and phlorizin binding studies on the same preparation. Moreover, an interesting observation that stems from the above discussion is that the K_i value of 15 μM found in our studies is close to one order of magnitude higher than the K_d values of phlorizin binding usually recorded in the rabbit [61] and dog [64] kidneys, and in LLC-PK_1 cells [39]. Indeed, part of the discrepancy with the latter studies may be accounted for by differences in assay conditions (temperature, Na^+ concentrations). Quite importantly, however, because the K_d values of phlorizin binding in the kidney are usually determined at equilibrium (incubation times of 5 min or more) while the K_i values of SGLT inhibition are determined under initial rate conditions, the question arises, then, as to what extent could those conflictory results (i) reflect the fact that phlorizin may bind to different conformational states of the transporter(s) under these two sets of experimental conditions or, alternatively, (ii) be a direct consequence of the phlorizin binding mechanism itself. In this respect, it should be noted that Toggenburger et al. [57] reported that large differences could be observed in the time course of phlorizin binding in renal *vs.* intestinal BBMV from rat and rabbit, and that the binding velocity appeared to correlate with the K_d and K_i values. Quite interestingly too, the apparent K_i values in the rabbit small intestine decreased from 40–50 μM at 0.1 sec to approx. 7 μM in the time interval 1.3–1.8 sec [57]. Those questions were specifically addressed in the following two papers [42–43] where it is shown that: (i) phlorizin binding studies in the whole rabbit kidney cortex appear homogeneous, (ii) the difference in K_d values observed under initial rate and equilibrium conditions is a characteristic feature of the phlorizin binding mechanism itself, and (iii) the K_d values of 12–30 μM estimated under initial binding conditions are in the range of the K_i value of 15 μM (Fig. 6) reported in this paper.

It is quite remarkable, then, that our K_d and K_i values: (i) lie within the range of 5–30 μM determined by Toggenburger et al. [57] in rabbit intestinal BBMV (under initial rate conditions at room temperature, and in the presence of a 100 mM inward Na^+-gradient, higher K_d values were observed at decreasing membrane potential while similar K_d and K_i values were estimated for phlorizin binding and phlorizin inhibition of glucose transport), (ii) are similar to those determined in rSGLT1 cRNA-injected oocytes (5–15 μM in [69]), but (iii) are lower and higher, respectively, than those reported for SAAT1-pSGLT2-mRNA (37 μM at −10 mV but decreasing to ≈ 16 μM at hyperpolarizing potentials of −70 to −110 mV in [35]) and Hu14-hSGLT2-mRNA (K_i ≈ 0.4 μM as could be calculated from the data of Kanai et al. [25]) injected oocytes. It can thus be concluded that our results on phlorizin inhibition of SGLT (and binding [42–43]) in rabbit renal BBMV are compatible with the known expression of rSGLT1 in the small intestine [21] and the kidney [14, 40–41], so that our kidney results are also compatible with the concept that HAG and LAG may represent two different transport modes through the same rSGLT1 protein. In the dimeric model of Chenu and Berteloot [13], a possible interpretation would be that phlorizin binding, in contrast to glucose and galactose binding during transport, would occur in the absence of significant cooperativity between subunits, as also suggested in the pig by the work of Koepsell et al. [29].

Indeed, it could be argued that our kinetic studies may not be able to distinguish close K_i values for the phlorizin inhibition of glucose transport through rSGLT1 and rSGLT2 proteins. This is true only within the 95% confidence intervals of the K_i values determined in Fig.

6 for the HAG (9.8–20.2 μM) and LAG (11.1–17.9 μM) pathways (*results not shown*). It could be argued as well that phlorizin interaction with a SGLT2 protein may vary quite widely from species to species, a possibility that cannot be readily evaluated at this time. Still, in both cases, should rSGLT2 represent the LAG transport pathway in our BBMV preparations, it can be stated that this transporter would have phlorizin binding properties similar to those of rSGLT1 in spite of a 27- and 55-fold difference in transport affinities for glucose and galactose, respectively (Table 2).

Temperature Studies

To fully appreciate the results of Fig. 7*A* showing similar E_a for the renal HAG and LAG pathways, let us first consider the temperature dependence of two closely related proteins like rSGLT1 and hSGLT1 (there is 84% identity and 94% similarity into the amino acid sequences of the two transporters [69]). From our earlier studies in human jejunal BBMV [38], and if we assume linearity of the Arrhenius plots over the range 20–35°C of temperatures, it would appear that the K_m of hSGLT1 is insensitive to temperature and that a low E_a of 11.0 $\text{kcal} \cdot \text{mol}^{-1}$ can be calculated from the $V_{\max}$ data. Clearly, the picture is quite different from that observed in rabbit jejunal BBMV [13] and discussed earlier, so that the important conclusion to be drawn from such a comparison is that closely related proteins may show very different responses to temperature. Accordingly, the temperature dependence (or the lack thereof) of the kinetic parameters and the E_a values estimated from them may essentially reflect a property of the kinetic mechanism itself. Indeed, Loo et al. [34] have shown salient differences in the rate constant values characterizing a similar kinetic mechanism of sugar transport through hSGLT1 and rSGLT1. Accordingly, it may be quite difficult to assume, from the similar E_a values implicated in a full catalytic cycle leading to glucose transport through the HAG and LAG pathways in the kidney (Fig. 7*A*), that the two transport routes would correspond to SGLT1 and SGLT2 (there is only 59% or 76% identity between Hu14/hSGLT2 and hSGLT1 [25, 68] or pSGLT2 and pSGLT1 [35], respectively). Rather, our temperature studies demonstrate a higher increase with temperature of the kinetic efficiency (*V/K* ratio) of LAG as compared to HAG. In the dimeric model of cotransport proposed by Chenu and Berteloot [13], this behavior could be interpreted as a decrease with increasing temperatures in the negative cooperativity associated with glucose binding to the subunits.

Summary and General Conclusions

In conclusion, when taken individually, the results presented in this paper do not resolve conclusively the issue of whether SGLT in the whole kidney cortex results from the expression in the proximal tubule of two independent transporters (rSGLT1 and rSGLT2) or from the expression of a unique transporter (rSGLT1) showing allosteric kinetics. When taken together, however, they do point out a number of inconsistencies as to: (i) the kinetic parameters of rSGLT1 expression in the small intestine [13] and cRNA-injected oocytes [45, 66] as compared to the kidney (this study), and (ii) the substrate specificity and the phlorizin inhibition characteristics usually associated with SGLT1 and SGLT2 activities [25, 35, 59–61]. One is thus left with either of the following two alternatives which are not necessarily mutually exclusive: (i) rSGLT1 and rSGLT2 are coexpressed in renal BBMV but structural similarities [35] give them a number of overlapping functional characteristics; (ii) rSGLT1 activity is somehow modulated, for example through association with (a) regulatory subunit(s), as would be compatible with the studies of Koepsell's group [30, 66], such as masking rSGLT2 expression. The first consideration may be difficult to reconcile with the conclusion that two closely related proteins like hSGLT1 and rSGLT1 present very different behavior relative to temperature effects in the small intestine when the HAG and LAG pathways show similar E_a for a full catalytic cycle in the kidney. The second consideration, however, in conjunction with the dimeric structure proposed by Koepsell et al. [29–30] and the kinetic features of the dimeric model proposed by Chenu and Berteloot [13], could well account for the results presented in these studies, as discussed above for each experiment. Still, the presence of (a) regulatory subunit(s) may complicate quite significantly the above picture since the binding of the subunit(s) to a dimeric SGLT1 may not be stoichiometric [30, 66]. It can thus be suggested that such a heteroassociation might also contribute quite significantly to sugar transport heterogeneity in the kidney proximal tubule.

This research was supported by grant MT-7607 from the Medical Research Council of Canada. N.O. was supported by a fellowship from the GRTM. The technical assistance of Mrs. C. Leroy has been greatly appreciated.

References

1. Barfuss, D.W., Schafer, J. 1981. Differences in active and passive glucose transport along the proximal nephron. *Am. J. Physiol.* **240:**F322–F332
2. Béliveau, R., Demeule, M., Ibnoul, K.H., Bergeron, M., Beauregard, G., Potier, M. 1988. Radiation-inactivation studies on brush-border-membrane vesicles. General considerations and application to the glucose and phosphate carriers. *Biochem. J.* **252:**807–813
3. Berteloot, A. 1984. Characteristics of glutamic acid transport by rabbit intestinal brush-border membrane vesicles. Effect of Na^+-, K^+-, and H^+-gradients. *Biochim. Biophys. Acta* **775:**129–140
4. Berteloot, A. 1986. Highly permeant anions and glucose uptake as

an alternative for quantitative generation and estimation of membrane potential differences in brush-border membrane vesicles. *Biochim. Biophys. Acta* **857:**180–188

5. Berteloot, A., Malo, C., Breton, S., Brunnette, M. 1991. A fast sampling, rapid filtration apparatus: principal characteristics and validation from studies of D-glucose transport in human jejunal brush-border membrane vesicles. *J. Membrane Biol.* **122:**111–125
6. Berteloot, A., Semenza, G. 1990. Advantages and limitations of vesicles for the characterization and kinetic analysis of transport systems. *Meth. Enzymol.* **192:**409–437
7. Birnir, B., Loo, D.D., Wright, E.M. 1991. Voltage-clamp studies of the Na^+/glucose cotransporter cloned from rabbit small intestine. *Pfluegers Arch.* **418:**79–85
8. Blank, M.E., Bode, F., Baumann, K., Diedrich, D.F. 1989. Computer analysis reveals changes in renal Na^+-glucose cotransporter in diabetic rats. *Am. J. Physiol.* **257:**C385–C396
9. Brasitus, T.A., Schachter, D., Mamouneas, T.G. 1979. Functional interactions of lipids and proteins in rat intestinal microvillus membranes. *Biochemistry* **18:**4136–4144
10. Brot-Laroche, E., Serrano, M., Delhomme, B., Alvarado, F. 1986. Temperature sensitivity and substrate specificity of two distinct Na^+-activated D-glucose transport systems in guinea pig jejunal brush border membrane vesicles. *J. Biol. Chem.* **261:**6168–6176
11. Centelles, J.J., Kinne, R.K.H., Heinz, E. 1991. Energy coupling of Na^+/glucose cotransport. *Biochim. Biophys. Acta* **1065:**239–249
12. Chen, X.-Z., Coady, M.J., Jackson, F., Berteloot, A., Lapointe, J.-Y. 1995. Thermodynamic determination of the Na^+:glucose coupling ratio for the human SGLT1 cotransporter. *Biophys. J.* **69:**2405–2414
13. Chenu, C., Berteloot, A. 1993. Allosterism and Na^+-D-glucose cotransport kinetics in rabbit jejunal vesicles: compatibility with mixed positive and negative cooperativities in a homo-dimeric or tetrameric structure and experimental evidence for only one transport protein involved. *J. Membrane Biol.* **132:**95–113
14. Coady, M.J., Pajor, A.M., Wright, E.M. 1990. Sequence homologies among intestinal and renal Na^+/glucose cotransporters. *Am. J. Physiol.* **259:**C605–C610
15. Crane, R.K. 1977. The gradient hypothesis and other models of carrier-mediated active transport. *Rev. Physiol. Biochem. Pharmacol.* **78:**99–159
16. Desjeux, J.-F. 1995. Congenital selective Na^+, D-glucose cotransport defect leading to renal glucosuria and congenital selective intestinal malabsorption of glucose and galactose. *In:* The Metabolic Basis of Inherited Diseases. C.R. Scriver, editor. pp. 3563–3580. McGraw-Hill, New York
17. De Smedt, H., Kinne, R. 1981. Temperature dependence of solute transport and enzyme activities in hog renal brush border membrane vesicles. *Biochim. Biophys. Acta* **648:**247–253
18. Dorando, F.C., Crane, R.K. 1984. Studies of the kinetics of Na^+ gradient-coupled glucose transport as found in brush-border membrane vesicles from rabbit jejunum. *Biochim. Biophys. Acta* **772:**273–287
19. Gerardi-Laffin, C., Delque-Bayer, P., Sudaka, P., Poirée, J.C. 1993. Oligomeric structure of the sodium-dependent phlorizin binding protein from kidney brush-border membranes. *Biochim. Biophys. Acta* **1151:**99–104
20. Harig, J.M., Barry, J.A., Rajendran, V.M., Soergel, K.H., Ramaswamy, K. 1989. D-glucose and L-leucine transport by human intestinal brush-border membrane vesicles. *Am. J. Physiol.* **256:**G618–G623
21. Hediger, M.A., Coady, M.J., Ikeda, T.S., Wright, E.M. 1987. Expression cloning and cDNA sequencing of the Na^+/glucose cotransporter. *Nature* **330:**379–381
22. Hediger, M.A., Turk, E., Wright, E.M. 1989. Homology of the human intestinal Na^+/glucose and *E. coli* Na^+/proline cotransporters. *Proc. Natl. Acad. Sci. USA* **86:**5748–5752
23. Hilden, S., Sacktor, B. 1982. Potential-dependent D-glucose uptake by renal brush border membrane vesicles in the absence of sodium. *Am. J. Physiol.* **242:**F340–F345
24. Horster, M.F., Stopp, M. 1986. Transport and metabolic functions in cultured renal tubule cells. *Kid. Int.* **29:**46–53
25. Kanai, Y., Lee, W.S., You, G., Brown, D., Hediger, M.A. 1994. The human kidney low affinity Na^+/glucose cotransporter SGLT2. *J. Clin. Invest.* **93:**397–404
26. Kimmich, G.A. 1990. Membrane potentials and the mechanism of intestinal Na^+-dependent sugar transport. *J. Membrane Biol.* **114:**1–27
27. Kinne, R., Murer, H., Kinne-Saffran, E., Thees, M., Sachs, G. 1975. Sugar transport by renal plasma membrane vesicles. *J. Membrane Biol.* **21:**375–396
28. Kippen, N., Hirayama, B., Klinenberg, J.R., Wright, E.M. 1979. Transport of p-aminohippuric acid, uric acid and glucose in highly purified rabbit renal brush border membranes. *Biochim. Biophys. Acta* **556:**161–174
29. Koepsell, H., Fritzsch, G., Korn, K., Madrala, A. 1990. Two substrate sites in the renal Na^+-D-glucose cotransporter studied by model analysis of phlorizin binding and D-glucose transport measurements. *J. Membrane Biol.* **114:**113–132
30. Koepsell, H., Spangenberg, J. 1994. Function and presumed molecular structure of Na^+-D-glucose cotransport systems. *J. Membrane Biol.* **138:**1–11
31. Kong, C-T., Yet, S.-F., Lever, J.E. 1993. Cloning and expression of a mammalian Na^+/amino acid cotransporter with sequence similarity to Na^+/glucose cotransporters. *J. Biol. Chem.* **268:**1509–1512
32. Lescale-Matys, L., Dyer, J., Scott, D., Freeman, T.C., Wright, E.M., Shirazi-Beechey, S.P. 1993. Regulation of the ovine intestinal Na^+/glucose cotransporter (SGLT1) is dissociated from mRNA abundance. *Biochem. J.* **291:**435–440
33. Lever, J.E. 1986. Expression of differentiated functions in kidney epithelial cell lines. *Miner. Electrol. Metab.* **12:**14–19
34. Loo, D.D.F., Hazama, A., Supplisson, S., Turk, E., Wright, E.M. 1993. Relaxation kinetics of the Na^+/glucose cotransporter. *Proc. Natl. Acad. Sci. USA* **90:**5767–5771
35. Mackenzie, B., Panayotova-Heiermann, M., Loo, D.D.F., Lever, J.E., Wright, E. 1994. SAAT1 is a low affinity Na^+/glucose cotransporter and not an amino acid transporter. *J. Biol. Chem.* **269:**22488–22491
36. Maenz, D.D., Chenu, C., Bellemare, F., Berteloot, A. 1991. Improved stability of rabbit and rat intestinal brush border membrane vesicles using phospholipase inhibitors. *Biochim. Biophys. Acta* **1069:**250–258
37. Malo, C. 1993. Ontogeny of Na^+/D-glucose cotransport in guinea-pig jejunal vesicles: only one system is involved at both 20°C and 35°C. *Biochim. Biophys. Acta* **1153:**299–307
38. Malo, C., Berteloot, A. 1991. Analysis of kinetic data in transport studies: new insights from kinetic studies of Na^+-D-glucose cotransport in human brush-border membrane vesicles using a fast sampling, rapid filtration apparatus. *J. Membrane Biol.* **122:**127–141
39. Moran, A., Davis, L.J., Turner, R.J. 1988. High affinity phlorizin binding to the LLC-PK_1 cells exhibits a sodium: phlorizin stoichiometry of 2:1. *J. Biol. Chem.* **263:**187–192
40. Morrisson, A.I., Panayotova-Heiermann, G., Feigl, B., Schölermann, B., Kinne, R.K.H. 1991. Sequence comparison of the sodium-D-glucose cotransport systems in rabbit renal and intestinal epithelia. *Biochim. Biophys. Acta* **1089:**121–123
41. Ohta, T., Isselbacher, K.J., and Rhoads, D.B. 1990. Regulation of

glucose transporters in LLC-PK$_1$ cells: effect of D-glucose and monosaccharides. *Mol. Cell. Biol.* **10:**6491–6499

42. Oulianova, N., Berteloot, A. 1996. Sugar transport heterogeneity in the kidney: two independent transporters or different transport modes through an oligomeric protein? 2. Phlorizin binding studies. *J. Membrane Biol.* (*submitted*)
43. Oulianova, N., Berteloot, A. 1996. Sugar transport heterogeneity in the kidney: two independent transporters or different transport modes through an oligomeric protein? 3. Mechanism of phlorizin binding and implications. *J. Membrane Biol.* (*submitted*)
44. Pajor, A.M., Hirayama, B.A., Wright, E.M. 1992. Molecular evidence for two renal Na^+/glucose cotransporters. *Biochim. Biophys. Acta* **1106:**216–220
45. Parent, L., Supplisson, S., Loo, D.D.F., Wright, E.M. 1992. Electrogenic properties of the cloned Na^+/glucose cotransporter: I. Voltage-clamp studies. *J. Membrane Biol.* **125:**49–62
46. Parent, L., Wright, E.M. 1993. Electrophysiology of the Na^+/glucose cotransporter. *Soc. Gen. Physiol. Ser.* **48:**263–281
47. Rabito, C.A. 1986. Sodium cotransport processes in renal epithelial cell lines. *Miner. Electrol. Metab.* **12:**32–41
48. Reizer, J., Reizer, A., Saier, M.H.Jr. 1994. A functional superfamily of sodium/solute symporters. *Biochim. Biophys. Acta* **1197:**133–166
49. Roigaard-Petersen, H., Jacobsen, C., Iqbal Sheikh, M. 1986. Characteristics of D-galactose transport systems by luminal membrane vesicles from rabbit kidney. *Biochim. Biophys. Acta* **856:**578–584
50. Scriver, S.R., Chesney, R.W., McInnes, R.R. 1976. Genetic aspects of renal tubular transport: Diversity and topology of carriers. *Kidney Int.* **9:**149–171
51. Semenza, G., Kessler, M., Hosang, M., Weber, J., Schmidt, U. 1984. Biochemistry of the Na^+-D-glucose cotransporter of the small intestine brush-border membranes: the state of the art in 1984. *Biochim. Biophys. Acta* **779:**343–379
52. Shirazi-Beechey, S.P., Hirayama, B.A., Wang, Y., Scott, D., Smith, M.W., Wright, E.M. 1991. Ontogenetic development of lamb intestinal sodium-glucose cotransporter is regulated by diet. *J. Physiol.* **437:**699–708
53. Silverman, M. 1991. Structure function of hexose transporters. *Annu. Rev. Biochem.* **60:**757–794
54. Silverman, M., Speight, P., Ho, L. 1993. Identification of two unique polypeptides from dog kidney outer cortex and outer medulla that exhibit different Na^+/D-glucose cotransport functional properties. *Biochim. Biophys. Acta* **1153:**43–52
55. Stevens, B.R., Fernandez, A., Hirayama, B., Wright, E.M., Kempner, E.S. 1990. Intestinal brush border membrane Na^+/glucose cotransporter functions in situ as a homotetramer. *Proc. Natl. Acad. Sci. USA* **87:**1456–1460
56. Takahashi, M., Malathi, P., Preiser, H., Jung, C.Y. 1985. Radiation inactivation studies on the rabbit kidney sodium-dependent glucose transporter. *J. Biol. Chem.* **260:**10551–10556
57. Toggenburger, G., Kessler, M., Semenza, G. 1982. Phlorizin as a probe of the small intestinal Na^+, D-glucose cotransporter. A model. *Biochim. Biophys. Acta* **688:**557–571
58. Turk, E. Zabel, B., Mundlos, S., Dyer, J., Wright, E.M. 1991. Glucose/galactose malabsorption caused by a defect in the Na^+/D-glucose cotransporter. *Nature* **350:**354–356
59. Turner, R.J., Moran, A. 1982. Heterogeneity of sodium-dependent D-glucose transport sites along the proximal tubule: evidence from vesicle studies. *Am. J. Physiol.* **242:**F406–F414
60. Turner, R.J., Moran, A. 1982. Stoichiometric studies of the renal outer cortical brush border membrane D-glucose transporter. *J. Membrane Biol.* **67:**73–80
61. Turner, R.J., Moran, A. 1982. Further studies of proximal tubular brush border membrane D-glucose transport heterogeneity. *J. Membrane Biol.* **70:**37–45
62. Turner, R.J., Kempner, E.S. 1982. Radiation inactivation studies of the renal brush-border membrane phlorizin-binding protein. *J. Biol. Chem.* **257:**10794–10797
63. Turner, R.J., Silverman, M. 1977. Sugar uptake into brush border vesicles from normal human kidney. *Proc. Natl. Acad. Sci. USA* **74:**2825–2829
64. Turner, R.J., Silverman, M. 1981. Interaction of phlorizin and sodium with the renal brush-border membrane D-glucose transporter: stoichiometry and order of binding. *J. Membrane Biol.* **58:**43–55
65. Umbach, J.A., Coady, M.J., Wright, E.M. 1990. Intestinal Na^+/glucose cotransporter expressed in *Xenopus* oocytes is electrogenic. *Biophys. J.* **57:**1217–1224
66. Veyhl, M., Spangenberg, J., Puschel, B., Poppe, R., Dekel, C., Fritzsch, G., Haase, W., Koepsell, H. 1993. Cloning of a membrane-associated protein which modifies activity and properties of the Na^+-D-glucose cotransporter. *J. Biol. Chem.* **268:**25041–25053
67. Vinay, P., Senecal, J., Noël, J., Chirinian, C., Vinay, M.C., Ammann, H., Boulanger, Y., Gougoux, A., Berteloot, A. 1991. Basolateral glucose transport in distal segments of the dog nephron. *Can. J. Physiol. Pharmacol.* **69:**964–977
68. Wells, R.G., Pajor, A.M., Kanai, Y., Turk, E., Wright, E.M., Hediger, M.A. 1992. Cloning of a human cDNA with similarity to the sodium-glucose cotransporter. *Am. J. Physiol.* **263:**F459–F465
69. Wright, E.M. 1993. The intestinal Na^+/glucose cotransporter. *Annu. Rev. Physiol.* **55:**575–589
70. Wright, E.M., Turk, E., Zabel, B., Mundlos, S., Dyer, J. 1991. Molecular genetics of intestinal glucose transport. *J. Clin. Invest.* **88:**1435–1440
71. You, G., Lee, W.-S., Barros, E.J.G., Kanai, Y., Huo, T.-L., Khawaja, S., Wells, R.G., Nigam, S.K., Hediger, M.A. 1995. Molecular characteristics of Na^+-coupled glucose transporters in adult and embryonic rat kidney, *J. Biol. Chem.* **270:**29365–29371